Supplementary Figure 1

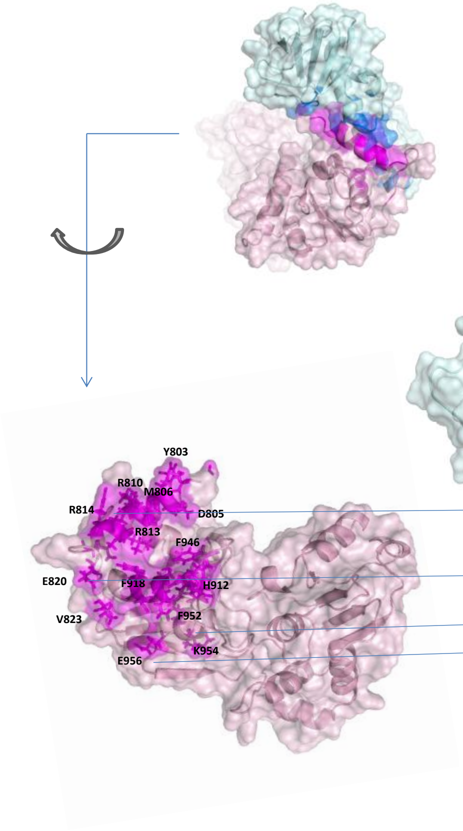

Interaction between domain 1A and the N-terminal domain in ToMV-Hel. The structures are shown as surface representations superpositioned on ribbon diagrams. The helicase core and the N-terminal domain are colored magenta and blue, respectively. The residues in one of the domains that interact with those in the other domain are shown as stick models and are labeled. The figure was created using pyMol (http://pymol.org/pymol).

Supplementary Table 2. Oligonucleotides used in this study.

Number	Name	Sequence (5'→ 3')
1	NcoI-L666-F	GCGCCATGGCCTCATACACTAGGAGCGAGGAG
2	NcoI-V802-F	GCGCCATGGCCGTATATTCTGATATGGCTAAACTC
3	PstI-stop-V801-R	GCGCTGCAGTTATACCGACTCAGAACTCACAGCC
4	PstI-stop-Q1116-R	GCGCTGCAGTTATTGAGTACCTGCATCTACTTTGTAC
5	NcoI-G699-F	GCGCCATGGCCGGCCCTCTTAAAGTTCAACAAATG
6	PstI-stop-A732-R	GCGCTGCAGTTAGGCTGTATCTTTTAGGATCTTCAC
7	SpeI-G699-F	GCGACTAGTAAAAATGGGCCCTCTTAAAGTTCAACAAATG
8	SalI-stop-A732-R	GCGGTCGACTTAGGCTGTATCTTTTAGGATCTTCAC

Restriction sites are underlined.

Supplementary Table3 Comparison of ToMV-Hel core structure with those of other SF1 helicases performed by the DALI server [1].

No.	PDB No.	Z score[a]	RMSD[b]	LALI[c]	NRES[d]	Number of identical residues (%)	Comment	Ref
1	2gk7-A	21.2	3.3	284	596	14	Upf1/SO$_4^2$ complex	2
2	1uaa-B	18.8	2.9	248	633	17	Rep/DNA complex	3
3	2gk6-A	18.6	3.2	281	602	15	Upf1/ADP complex	2
4	2is4-B	18.5	3.1	251	632	14	UvrD/AMPPNP complex	4
5	1pjr-A	18.5	3.3	251	623	17	Free PcrA	5
6	2gk6-B	18.5	3.2	282	602	15	Upf1/ADP complex	2
7	2is4-A	18.4	3.1	248	646	15	UvrD/AMPPNP complex	4
8	2is1-A	18.1	2.9	248	649	15	UvrD/SO$_4^2$ complex	4
9	2is1-B	18.0	2.9	247	624	15	UvrD/SO$_4^2$ complex	4
10	2xzp-A	17.9	3.1	287	621	14	Free Upf1(ΔCH)	6
11	2is2-B	17.8	3.0	245	642	15	UvrD NTP-free	4
12	2xzo-A	17.7	3.7	287	613	15	Upf1(ΔCH)/RNA/ADP·AlF$_4$ complex	6
13	2gjk-A	17.6	3.4	284	614	14	Upf1/AMPPNP complex	2
14	2wjy-A	17.4	3.3	287	773	14	Upf1/Upf2 complex	7
15	2is6-A	17.4	3.1	248	654	15	UvrD/ADP·MgF$_3$ complex	4
16	2wjv-A	16.2	3.4	287	772	14	Upf1/Upf2 complex	7
17	2xzl-A	16.2	3.5	281	756	14	Upf1/RNA/ADP·AlF$_4$ complex	6
18	3gpl-B	15.2	3.7	234	516	16	RecD2/ADPNP/ssDNA complex	8
19	3gpl-A	15.2	3.7	235	516	16	RecD2/ADPNP/ssDNA complex	8
20	3lfu-A	15.1	3.1	246	633	15	UvrD/SO$_4^{2-}$ complex	9
21	1qhg-A	15.1	3.2	251	622	17	Pcr/ATP complex	10
22	3pjr-A	15.0	2.8	250	646	17	PcrA/ATP/DNA complex	11
23	1uaa-A	15.0	3.0	248	636	16	Rep/DNA complex	3
24	2wjv-B	14.7	3.3	284	768	14	Upf1/Upf2 complex	7
25	2is2-A	14.7	3.1	246	642	15	UvrD NTP-free	4
26	3e1s-A	14.7	3.2	225	517	16	RecD2	12
27	2is6-B	14.2	3.1	248	652	15	UvrD/ADP·MgF$_3$ complex	4
28	3gp8-A	13.7	3.5	231	551	16	RecD2/ADPNP/ssDNA complex	8
29	1w36-D	13.6	4.1	230	538	15	RecD2 in RecBCD/DNA complex	13

30	1w36-G	13.5	4.0	228	538	15	RecD2 in RecBCD/DNA complex	13
31	3k70-G	13.5	4.2	229	547	16	RecD2/DNA comp	12
32	3k70-D	12.8	4.1	228	547	16	RecD2/DNA comp	12
33	3k70-B	12.0	3.7	248	1155	18	RecD2/DNA comp	12
34	3k70-E	11.9	3.7	248	1155	18	RecD2/DNA comp	12
35	3rc3-A	11.9	3.6	210	607	17	Suv3/RNA complex	
36	3i5y-A	11.9	5.4	168	509	7	Mss116p (DEAS-box)	14
37	2p6r-A	11.9	4.0	212	683	15	SF2 helicase	15
38	1w36-B	11.7	3.7	246	1158	18	RecD2 in RecBCD/DNA complex	13
39	2pjr-F	11.7	2.9	194	544	16	PcrA/SO_4^{2-}/DNA complex	11
40	2pjr-A	11.7	3.0	195	542	16	PcrA/SO_4^{2-}/DNA complex	11
41	1w36-E	11.7	3.7	247	1158	18	RecD2 in RecBCD/DNA complex	13
42	3g0h-A	11.7	3.7	219	408	14	DDX19 (DEXD/H-box)	16
43	3fht-A	11.7	3.8	217	392	14	Dbp5/AMPPNP/RNA complex	17
44	3rc8-A	11.6	3.8	206	609	17	Suv3/RNA complex	
45	3fht-B	11.6	3.8	218	387	14	Dbp5/AMPPNP/RNA complex	17
46	2p6n-B	11.5	2.5	116	158	10	DDX41 (DEAD-box)	18
47	2p6n-A	11.4	2.6	116	160	10	DDX41 (DEAD-box)	18
48	3rrn-A	11.4	3.9	219	389	13	DEAD-box	19
49	3pex-A	11.4	3.9	219	389	13	D90Dbp5(L327V)/InsP6/Gle1(H337R) /ADP complex	19
50	2va8-A	11.4	4.4	212	693	9	Hel308	20

Rows highlighted by yellow, blue, and green contain Uvr/Rep-type, Upf1-like, and Pif1-like SF1 helicases, respectively.

[a] The Z score is composed of several evaluations, including rmsd and the number of residues matched. A score less than 2.0 means that the two structures do not significantly match, while a score greater than 10.0 shows a very strong match.

[b] Root-mean-square deviation of the three-dimensional alignment.

[c] Number of residues in the matched structure.

[d] Number of aligned residues.

References

1. Holm, L. & Rosenstrom, P. Dali server: conservation mapping in 3D. *Nucleic Acids Res* **38**, W545-9 (2010).
2. Cheng, Z., Muhlrad, D., Lim, M.K., Parker, R. & Song, H. Structural and functional insights into the human Upf1 helicase core. *EMBO J* **26**, 253-64 (2007).
3. Korolev, S., Hsieh, J., Gauss, G.H., Lohman, T.M. & Waksman, G. Major domain swiveling revealed by the crystal structures of complexes of E. coli Rep helicase bound to single-stranded DNA and ADP. *Cell* **90**, 635-47 (1997).
4. Lee, J.Y. & Yang, W. UvrD helicase unwinds DNA one base pair at a time by a two-part power stroke. *Cell* **127**, 1349-60 (2006).
5. Subramanya, H.S., Bird, L.E., Brannigan, J.A. & Wigley, D.B. Crystal structure of a DExx box DNA helicase. *Nature* **384**, 379-83 (1996).
6. Chakrabarti, S., Jayachandran, U., Bonneau, F., Fiorini, F., Basquin, C., Domcke, S., Le Hir, H. & Conti, E. Molecular mechanisms for the RNA-dependent ATPase activity of Upf1 and its regulation by Upf2. *Mol Cell* **41**, 693-703 (2011).
7. Clerici, M., Mourão, A., Gutsche, I., Gehring, N.H., Hentze, M.W., Kulozik, A., Kadlec, J., Sattler, M. & Cusack, S. Unusual bipartite mode of interaction between the nonsense-mediated decay factors, UPF1 and UPF2. *EMBO J* **28**, 2293-306 (2009).
8. Saikrishnan, K., Powell, B., Cook, N.J., Webb, M.R. & Wigley, D.B. Mechanistic basis of 5'-3' translocation in SF1B helicases. *Cell* **137**, 849-59 (2009).
9. Jia, H., Korolev, S., Niedziela-Majka, A., Maluf, N.K., Gauss, G.H., Myong, S., Ha, T., Waksman, G. & Lohman, T.M. Rotations of the 2B Sub-domain of E. coli UvrD Helicase/Translocase Coupled to Nucleotide and DNA Binding. *J Mol Biol* **411**, 633-48 (2011).
10. Soultanas, P., Dillingham, M.S., Velankar, S.S. & Wigley, D.B. DNA binding mediates conformational changes and metal ion coordination in the active site of PcrA helicase. *J Mol Biol* **290**, 137-48 (1999).
11. Velankar, S.S., Soultanas, P., Dillingham, M.S., Subramanya, H.S. & Wigley, D.B. Crystal structures of complexes of PcrA DNA helicase with a DNA substrate indicate an inchworm mechanism. *Cell* **97**, 75-84 (1999).
12. Saikrishnan, K., Griffiths, S.P., Cook, N., Court, R. & Wigley, D.B. DNA binding to RecD: role of the 1B domain in SF1B helicase activity. *EMBO J* **27**, 2222-9 (2008).
13. Singleton, M.R., Dillingham, M.S., Gaudier, M., Kowalczykowski, S.C. & Wigley, D.B. Crystal structure of RecBCD enzyme reveals a machine for processing DNA breaks.

Nature **432**, 187-93 (2004).

14. Del Campo, M. & Lambowitz, A.M. Structure of the Yeast DEAD box protein Mss116p reveals two wedges that crimp RNA. *Mol Cell* **35**, 598-609 (2009).
15. Büttner, K., Nehring, S. & Hopfner, K.P. Structural basis for DNA duplex separation by a superfamily-2 helicase. *Nat Struct Mol Biol* **14**, 647-52 (2007).
16. Collins, R., Karlberg, T., Lehtiö, L., Schütz, P., van den Berg, S., Dahlgren, L.G., Hammarström, M., Weigelt, J. & Schüler, H. The DEXD/H-box RNA helicase DDX19 is regulated by an {alpha}-helical switch. *J Biol Chem* **284**, 10296-300 (2009).
17. von Moeller, H., Basquin, C. & Conti, E. The mRNA export protein DBP5 binds RNA and the cytoplasmic nucleoporin NUP214 in a mutually exclusive manner. *Nat Struct Mol Biol* **16**, 247-54 (2009).
18. Schutz, P., Karlberg, T., van den Berg, S., Collins, R., Lehtio, L., Högbom, M., Holmberg-Schiavone, L., Tempel, W., Park, H.W., Hammarström, M., Moche, M., Thorsell, A.G. & Schüler, H. Comparative structural analysis of human DEAD-box RNA helicases. *PLoS One* **5**, e12791 (2010).
19. Montpetit, B., Thomsen, N.D., Helmke, K.J., Seeliger, M.A., Berger, J.M. & Weis, K. A conserved mechanism of DEAD-box ATPase activation by nucleoporins and InsP6 in mRNA export. *Nature* **472**, 238-42 (2011).
20. Richards, J.D., Johnson, K.A., Liu, H., McRobbie, A.M., McMahon, S., Oke, M., Carter, L., Naismith, J.H. & White, M.F. Structure of the DNA repair helicase hel308 reveals DNA binding and autoinhibitory domains. *J Biol Chem* **283**, 5118-26 (2008).